Effect of Plasma Scale Length on Multi-MeV Proton Production by Intense Laser Pulses

A. J. Mackinnon,[1] M. Borghesi,[2] S. Hatchett,[1] M. H. Key,[1] P. K. Patel,[1] H. Campbell,[3] A. Schiavi,[3] R. Snavely,[1] S. C. Wilks,[1] and O. Willi[3]

[1]*Lawrence Livermore National Laboratory, Livermore, California 94550*
[2]*Queens University, Belfast, United Kingdom*
[3]*Imperial College of Science, Technology and Medicine, London, England*

(Received 14 July 2000; revised manuscript received 26 December 2000)

The influence of the plasma density scale length on the production of MeV protons from thin foil targets irradiated at $I\lambda^2 = 5 \times 10^{19}$ W cm^{-2} has been studied. With an unperturbed foil, protons with energy >20 MeV were formed in an exponential energy spectrum with a temperature of 2.5 ± 0.3 MeV. When a plasma with a scale length of 100 μm was preformed on the back of the foil, the maximum proton energy was reduced to <5 MeV and the beam was essentially destroyed. The experimental results are consistent with an electrostatic accelerating mechanism that requires an ultrashort scale length at the back of the target.

DOI: 10.1103/PhysRevLett.86.1769 PACS numbers: 52.50.Jm, 52.38.Ph, 52.40.Mj, 52.70.Kz

The generation of multi-MeV proton and ion beams from plasmas produced by the interaction of an ultrashort laser pulse is a rapidly growing research area. Such particle sources are interesting, in part, because they have potential for important applications in areas such as proton accelerators [1], investigations of material structures [2], proton radiography [3], and the possible production of short-lived radioisotopes for medical purposes [4]. Early work using long pulse CO_2 lasers at an irradiance-wavelength product $I\lambda^2 \sim 5 \times 10^{17}$ W cm^{-2} has been ongoing from the early 1970s [5–9]. More recent work at $I\lambda^2 > 5 \times 10^{18}$ W cm^{-2} has shown proton production up to 5 MeV [10,11]. The production of multi-MeV particles in distinct collimated beams has been observed in a number of very recent experiments. In particular, Clark *et al.* [12] observed protons with energies up to 20 MeV emitted into a half angle of 30° in the forward direction from a 110 μm thick aluminum foil that was irradiated by a 1 ps, 1 μm laser pulse, at 5×10^{19} W cm^{-2}. In another experiment at somewhat lower laser irradiance ($I\lambda^2 = 2 \times 10^{18}$ W cm^2), $\lambda = 0.527$ μm, on 1.5 μm Al and plastic foils, Maksimchuk *et al.* [13] also observed protons accelerated in the forward direction to a maximum energy of 2 MeV.

The interpretation for both of these experiments was that the protons were generated and accelerated from hydrogen impurities present in the plasma at the *front* of the target.

This interpretation appears incompatible with results obtained from experiments performed on the petawatt laser at Lawrence Livermore National Lab, which produced forward going protons with energies up to 50 MeV in a collimated beam from 125 μm thick, gold and plastic targets [14]. These experiments were consistent with proton acceleration of impurity layers from the *back* of the target. Hatchett *et al.* [15] have interpreted these results in terms of an electrostatic acceleration mechanism.

Briefly, the electrostatic mechanism is as follows. The laser-matter interaction at the front of the target produces a large number of hot electrons capable of penetrating several times through the target. Typically, their number and energy (kT_H) and the target capacitance are such that only a small fraction escapes before the target is sufficiently charged that escape is near impossible. The remaining hot electrons then bounce back and forth, ionizing the matter as they go, and ultimately fill the target volume and a thin Debye sheath surrounding it. The cold electrons sag slightly inward isolating a positive surface charge density whose field confines the hot electrons in the sheath. If the matter density is a step function at the surface, the well-known result [6–9] is a field $E \approx \sqrt{2}\, kT_H/e\ell_D$, where ℓ_D is the Debye length for the hot temperature, number, and volume currently occupied. Typically, ℓ_D is of order a micron in these experiments, so the electrostatic sheath fields are of order megavolts/micron, which can accelerate protons to the energies MeV energies observed. On the other hand, if the matter (ion) density at the surface has an initial scale length $\ell_i > \ell_D$, then the hot electron density will follow the matter density down until the *local* Debye length exceeds the ion density scale length, and at that point the hot electron sheath will separate. The net result is that on any target surface we have $E \approx \sqrt{2}\, kT_H/e \max(\ell_D, \ell_i)$. Particle-in-cell (PIC) modeling confirms these ideas: Efficient production of high-energy protons depends on a large hot electron temperature and an initially, short ion density scale length at the back of the target [16]. Thus, this electrostatic model makes a clear prediction that an initial density scale length of order 100 μm, *on the back of the target,* will result in orders of magnitude less proton acceleration, compared to an unperturbed back, while there should be little or no effect if the protons are accelerated on the front.

This Letter reports on experimental observations of the interaction of ultraintense laser pulses with aluminum (Al) and Al coated Mylar (AlCHO) foils with and without preformed plasmas on the back surface of the foil. Particle detectors were used to diagnose the energy characteristics

of the ions produced during the interaction. Time-resolved optical probing was used to measure the preformed plasma on both the front and the rear of the foils. The proton beam was found to depend strongly on the plasma scale length at the back of the target. The observed influence of the peak and mean ion energies on scale length were found to be consistent with the analytic electrostatic ion model and computational modeling, which both indicated that the acceleration occurred predominantly at the back surface of the target.

The experiment was performed at the Rutherford Appleton Laboratory using the Vulcan Nd:glass laser operating in the chirped pulse amplification (CPA) mode [17]. The targets were Al foils, 1 mm side, 1 cm long, and 25 μm thick (i.e., in the laser propagation direction). The 1.054 μm CPA interaction pulse, 1 ps in duration, with an energy of about 50 J was focused by an $f/3.5$ off-axis parabola at normal incidence onto the center of the coated side of the target. The focal spot was between 8 and 10 μm full width at half maximum (FWHM), which contained 30%–40% of the energy, giving peak intensity of 5×10^{19} W/cm^2. A fraction of the CPA pulse was compressed with a separate pair of gratings to a duration of 1 ps (FWHM); frequency quadrupled using two potassium dihydrogen phosphate crystals and used as a temporally independent probe. The probe, a collimated beam with a diameter of about 3 mm, propagated through the target along a direction transverse to the interaction axis. The relative timing of probe and interaction pulse was controlled to within a few picoseconds. A microscope objective, operating at $f/4$, imaged the target with a magnification of 55 onto UV sensitive photographic film resulting in a spatial resolution of 2–3 μm in the target plane.

The main experimental diagnostic of the proton flux produced during the interactions was radiochromic film (RCF). This consists of an organic dye sandwiched between two or more layers of plastic with a total thickness of 250 μm [14]. The dye is sensitive to the total radiation dose (x rays, ions, and electrons), and the optical density has been absolutely calibrated to give the absorbed radiation dose in krads (10^{-2} J/g). Typically, layers of RCF were placed at a known distance behind the target, aligned so that the face of the film was perpendicular to the normal to the back of the target. Al filters were placed in front of the first layer of film giving a minimum, detectable proton energy of 3.5 MeV. In some shots, each film layer acted as an energy filter for the subsequent layer while in others the RCF were separated by additional layers of Mylar. These intermediate Mylar layers were subsequently etched to reveal particle tracks. This provided a complementary method of measuring the energy deposited by the protons, analogous to the use of CR39 particle detectors [10,12]. In addition to these particle diagnostics, interferograms of the target were made 5 ps before the incidence of the interaction pulse, thus allowing the preformed plasma scale length to be measured up to a density of 5×10^{20} cm^{-3}.

The preformed plasma was created by focusing a 600 ps duration laser pulse at $\lambda = 0.527$ μm onto the back surface of the foil with an $f/10$ lens. The energy, focal spot, and relative timing of the preforming laser pulse (from here on referred to as the preforming beam) were all controlled on a shot to shot basis. For most shots, the energy on target was 10 J within a focal spot of 300 μm (FWHM), and the preforming beam started 250 ps before the interaction pulse, thus giving a mean intensity on target of 3×10^{13} W cm^{-2}. Figure 1 shows a schematic of the experimental arrangement.

Data from the second RCF layer of a typical proton beam generated from an Al foil with an unperturbed back surface is shown in Fig. 2(a). The proton beam is the distinct feature at the top edge of the film surrounded by a diffuse background due to energetic electrons. Only half of the proton beam is visible on the RCF because the preforming beam was incident from directly above the film pack, which, consequently, had to be lowered to allow all of the preforming beam to hit the back of the target. The response of each film is determined by the energy deposition of the protons within the active layer: For ions, the majority of the energy is deposited towards the end of the stopping range (the Bragg peak) [18]. The response of each RCF layer to high-energy protons has been determined using Monte Carlo modeling of the deposited energy by the particles. Each film responds to ions within an energy band of less than 1 MeV. The data from the second layer shown in Fig. 2(a) represents proton energies between 9.5–10 MeV. For the unperturbed case, a strong proton signal was observed out to the fifth RCF layer, which corresponded to proton energy of 21.7 MeV. This cutoff is in quantitative agreement with the data presented by Clarke *et al.* [12], which were obtained using the same Vulcan laser facility.

The situation was very different when the preforming beam was incident on the back surface of the foil, 250 ps prior to the arrival of the interaction pulse. The RCF data for this case is shown in Fig. 2(b). It can be seen that there is no evidence of a proton beam on the second RCF layer. In fact, there was no evidence of protons or ions after the first RCF layer. This means that there were no protons above an energy of 5 MeV. The same effect was

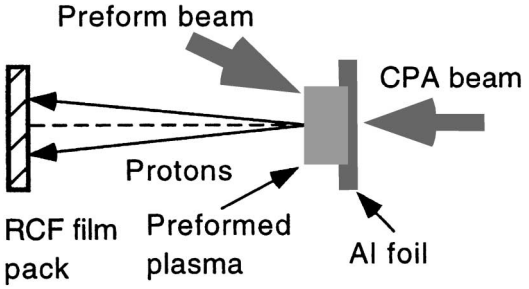

FIG. 1. Schematic of the experimental arrangement. The CPA beam is incident from the front and the preforming beam is incident from above and behind the target.

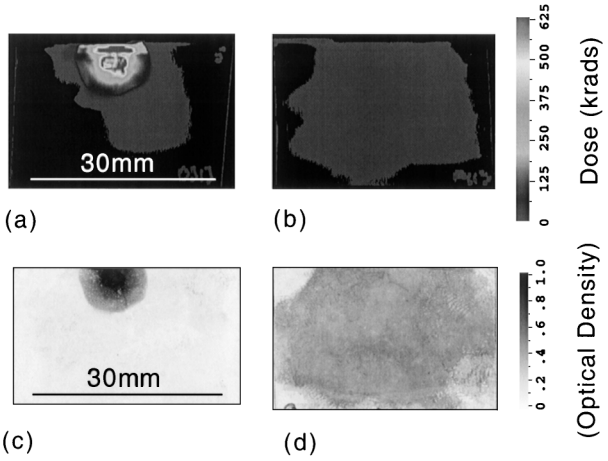

FIG. 2. Radiochromic film data for proton energies between 9.5–10 MeV: (a) an unperturbed target (b) with a 100 μm ion density scale length plasma on the back of the Al target. (c) Image of proton tracks in Mylar corresponding to the case with no preformed plasma and (d) corresponding to the preformed plasma case.

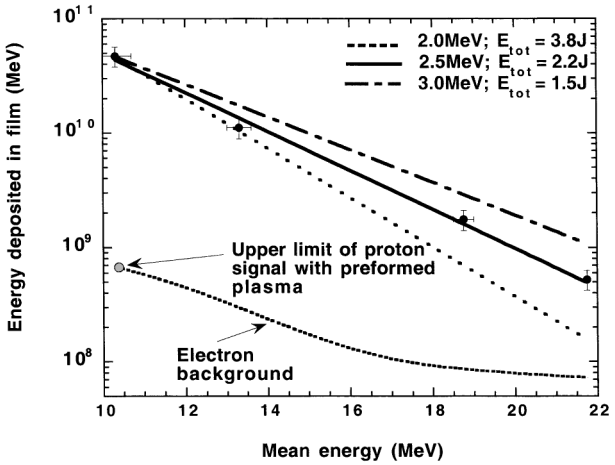

FIG. 3. Proton energy spectrum deconvolved from the RCF data shown in Fig. 2(a) and a single point representing the upper limit for a proton signal corresponding to the case of a preformed plasma on the back of the target, shown in Fig. 2(b).

also observed on the AlCHO targets, which were arranged with the Al side facing towards the CPA and the CHO side towards the preforming beam. This effect was reproducible (it was observed 3 times from three shots). Further confirmation of the greatly reduced proton signal in the preformed plasma case was obtained by etching the three Mylar layers that were between the first two RCF films. Images of the second etched Mylar layer for the unperturbed and preformed plasma cases are shown in Figs. 2(c) and 2(d). It is clear from comparing these images with their respective images in Figs. 2(a) and 2(b) that there is a one-to-one correspondence between the track features in the etched Mylar and the RCF data. For the unperturbed case, in each layer the track density within the proton beam is very high and the signal falls off very sharply at the edge region of the spot. In contrast, for the preformed plasma case, the track density is high only on the first Mylar layer and it dropped off to noise levels on the second Mylar layer.

The energy deposited within each film layer can be extracted from the absolutely calibrated film. By doing this for each film layer and fitting an exponential energy spectrum, an estimate of the mean and total proton energy can be extracted from the film data [14,15]. Figure 3 shows the energy deposited (in MeV) in the film as a function of proton energy for both cases. For the unperturbed foil, the plot is for all RCF layers apart from the first. The best fit to the data in these RCF layers is shown in Fig. 3. The mean proton energy of the exponential fit is 3.75 $\pm$ 0.3 MeV with a total energy of 2.2 J in an equivalent Maxwellian with a temperature of 2.5 MeV. For the preformed plasma case, it was not possible to fit a proton energy spectrum using this method because a signal above the background was detected only on the first layer of RCF. The film in this layer was saturated for both the unperturbed and preformed plasma cases so these layers did not provide useful data. One can, however, compare the energy deposited in the second RCF layer to the corresponding signal in the unperturbed foil case. As there is no signal visible due to protons on the second RCF layer, an upper limit can be placed if it is assumed that the proton signal is just less than the electron background. The background level, shown in Fig. 3, is a factor of 100 lower than the corresponding signal produced from the unperturbed foil. For the signal to be this strongly reduced, either the mean energy of the proton beam was reduced to sub-MeV levels and/or the production efficiency was affected by the preformed plasma on the back surface of the target.

Interferograms of the preformed plasma immediately before the arrival of the interaction pulse are shown in Figs. 4(a) and 4(b). In case 4(b), the plasma is clearly visible on the back of the foil, extending for 100 μm from the original target position, with a diameter of 300 μm, which is much larger than the interaction focal spot, and with a $1/e$ density scale length of 100 μm. In both cases, a small preplasma is visible on the front of the target with a scale length of a few μm: This is entirely due to the generic prepulse of the interaction (CPA) pulse. It is clear from these images that, apart from this generic preplasma region, the original target surface at the front is still intact. This is important as it shows the preforming beam on the back did not change the laser plasma interaction at the front of the target, which was still dominated by the conditions prevailing in the preplasma created by the generic prepulse.

If the protons were accelerated from the front rather than the back of the target, then a low temperature preformed plasma ($kT_e \sim 500$ eV) on the back surface of the target should not significantly disrupt 5–20 MeV protons or electrons. However, to test this hypothesis, a two target experiment was performed. Two identical targets were used:

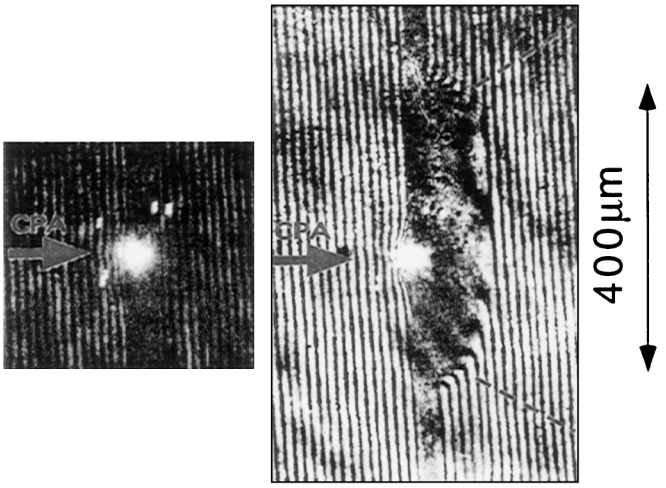

(a) (b)

FIG. 4. Interferograms of the preformed plasma for 2(a) and 2(b). In (a) plasma density scale length at the back of the target is less than the measurement resolution, while in (b) the scale length at the back of the target is 100 μm.

The first, which produced the protons, was an unperturbed 25 μm foil, as previously described. A preformed plasma with similar characteristics to that used in the first experiment was created on the back of the second foil, which was placed 500 μm behind the proton producing target. The proton beam appeared to be essentially unperturbed by this sort of preformed plasma on the second target.

These observations are entirely consistent with the electrostatic acceleration mechanism described above. If it is assumed that 40% of the incident laser energy is absorbed into hot electrons with a mean energy of 1.5 MeV and that these electrons fill the majority of the 25 μm thick target (a volume of $300 \times 300 \times 25$ μm), then $\ell_D \sim 1.6$ μm. For a target with an unperturbed back surface $E \sim 1.3$ MeV/micron, protons are accelerated to a maximum energy of 20 MeV by the end of the laser pulse by such a field. If, however, the scale is set by the 100 μm ion density scale length of the preformed plasma, then the maximum proton energy will be only in the few MeV range, as observed experimentally. One-dimensional PIC code simulations of this effect, which support this simple analytical model, have recently been published [16]. In these simulations, the influence of the density scale length of the back of the target on the peak and mean accelerated ion energy was investigated. For an initial hot electron temperature of 1 MeV and a step function at the back of the target (a plasma density scale length <0.05 μm), ions were found to be accelerated to 21 MeV by the end of the pulse. However, when the ion density scale length was increased from 0.05 to 14 μm, the peak ion energy was reduced to 5 MeV. This is in qualitative agreement with these experimental observations, where no protons above 3.5 MeV were observed for the longer scale length 100 μm produced in this experiment.

In conclusion, the acceleration of energetic protons from thin foil targets has been studied as the ion density scale length at the back of the target was varied. The maximum energy and efficiency of acceleration was found to depend very strongly on the existence of a short density scale length on the back surface of the target. The experimental observations were fully consistent with an electrostatic acceleration mechanism [15] and PIC code simulations [16]. This result is also important because it directly demonstrates that manipulation of the back surface of the target can significantly modify the energy and spatial distribution of the protons. Such modifications could conceivably be used to concentrate the proton/ion beam locally in a specific spatial region, which would be very useful for many potential applications.

The authors acknowledge the excellent staff of the Central Laser Facility. This work was funded by ESPRC/MoD grants and also under the auspices of the U.S. Department of Energy by the Lawrence Livermore National Laboratory under Contract No. W-7405-ENF-48.

[1] J. M. de Conto, J. Phys. (Paris) IV **9**, 115 (1999).
[2] D. S. Gemmel, Rev. Mod. Phys. **46**, 129 (1974).
[3] N. S. P. King *et al.,* Nucl. Instrum. Methods Phys. Res., Sect. A **424**, 84 (1999).
[4] J. Raloff, Science News **156**, 257 (1999).
[5] S. J. Gitomer, Phys. Fluids **29**, 2679 (1986).
[6] J. E. Crow, P. L. Auer, and J. E. Allen, J. Plasma Phys. **14**, 65 (1975).
[7] J. Denavit, Phys. Fluids **22**, 1385 (1979).
[8] Y. Kichimoto, K. Mima, T. Watanabe, and K. Nishikawa, Phys. Fluids **26**, 2308 (1983).
[9] J. S. Pearlman and R. L. Morse, Phys. Rev. Lett. **40**, 1652 (1978).
[10] A. P. Fews *et al.,* Phys. Rev. Lett. **73**, 1801 (1994).
[11] F. N. Beg *et al.,* Phys. Plasmas **4**, 447 (1997).
[12] E. L. Clark *et al.,* Phys. Rev. Lett. **84**, 670 (2000).
[13] A. Maksimchuk *et al.,* Phys. Rev. Lett. **84**, 4108 (2000).
[14] R. A. Snavely *et al.,* Phys. Rev. Lett. **85**, 2945 (2000).
[15] S. P. Hatchett *et al.,* Phys. Plasmas **7**, 2076 (2000).
[16] S. C. Wilks *et al.,* Phys. Plasmas **8**, 542 (2001).
[17] C. N. Danson *et al.,* J. Mod. Opt. **45**, 1653 (1998).
[18] A. Caruso and V. A. Pais, Nucl. Fusion **36**, 745 (1996).